Fiber ring laser based on Side-polished fiber MZI for enhancing refractive index and torsion measurement

Wan Bo, Bin Liu*, Juan Liu, Xing-Dao He, Jinhui Yuan and Qiang Wu

***Abstract*—A fiber ring laser based on a side-polish fiber Mach-Zehnder interferometer (MZI) for effective improving refractive index (RI) and torsion sensing is proposed and investigated. The side-polished fiber MZI sensor can not only enhance the evanescent wave but also break circular symmetry of optical fiber face section, so it can be used for the surrounding RI and torsion sensing. A spectrum 3 *dB* bandwidth of less than 0.15 *nm* has been achieved which makes the fiber ring laser torsion sensing system to have higher measurement resolution. Experiment results show that the RI and torsion sensitivity of proposed sensor is dependent on the polish depth: the thicker the polish depth, the higher the sensitivity. For a sensor with side polish depth of 47 μm, the measured RI sensitivity reaches -81.36 *nm*/RIU, the torsion sensitivity is as high as -0.019nm/^{O}, the sensitivity converted to torsional rate is -0.267 $nm/(rad.m^{-1})$.**

***Index Terms*—Erbium-doped fiber ring laser; Mach-Zehnder interference; Side-polished fiber; refractive index (RI) sensing; torsion sensing**

I. Introduction

In recent years, tunable erbium-doped fiber ring lasers have been comprehensively studied due to their great potential in space communication and fiber sensing[1]. The in-fiber Mach-Zehnder interferometer (MZI), which is composed of two interference arms integrated in an optical fiber, is widely used in optical fiber sensor, optical filter and optical fiber communication [2-4]. Therefore, researchers recently proposed to combine the erbium-doped ring cavity laser with the in-fiber MZI to construct a fiber laser sensor based on the in-fiber MZI [5-7]. The MZI modal not only has a filter effect, but also the passband of this filter is affected by the external environment [8], and thus is used in temperature [9], magnetic field [10,11], chemical gas [12], liquid concentration [13], refractive index (RI) [14,15], curvature [16,17], torque [18,19,20] and other factors detection [21].

This work was jointly supported by National Natural Science Foundation of China (NSFC) (11864025, 62175097 and 62065013); Natural Science Foundation of Jiangxi Province (Grant No. 20212BAB202024), Key R&D Projects of the Ministry of Science and Technology of China (2018YFE0115700). (Correspondence authors: Bin Liu, Qiang Wu and Jinhui Yuan)

Wan Bo, Bin Liu, Juan Liu, Xing-Dao He and Qiang Wu are with Key Laboratory of Opto-Electronic Information Science and Technology of Jiangxi Province, Nanchang Hangkong University, Nanchang 330063, China (e-mail: Baiwan12306@163.com; liubin_d@126.com; 18042@nchu.edu.cn; hxd@nchu.edu.cn; qiang.wu@northumbria.ac.uk). Qiang Wu is also with Faculty of Engineering and Environment, Northumbria University, Newcastle Upon Tyne NE1 8ST, UK.

Jinhui Yuan is with the Research Center for Convergence Networks and Ubiquitous Services, University of Science & Technology Beijing, Beijing 100083, China. (e-mail: yuanjinhui81@163.com).

On the other hand, side-polish optical fiber sensors have attracted wide research interests [22-24]. The side-polished fiber has a strong evanescent field, enhance the interference effect and polishing will also destroy the original symmetry of fiber structure, making the fiber more sensitive to changes such as axial force, RI [25] and temperature [26].

There are multiple peaks and valleys in the interference spectrum of a traditional optical fiber sensing system, and the 3-dB bandwidth is normally large, which is difficult to read the wavelength accurately and thus may lead to low measurement resolution and accuracy [27]. An optical fiber laser sensing system has a narrow full width at half maximum (FWHM) and high signal-to-noise ratio, whose wavelength can be measured accurately and thus has high sensing accuracy and resolution [28]. Yang et al. inserted a MZI based on Fiber Bragg grating into the fiber laser, which improves the detection limit and resolution of the sensor and is used to measure the surrounding RI and temperature [29]. Jiang et al. proposed an microcavity MZI fiber laser refractometer based on multi-mode fiber assistance, and constructed an open microcavity encapsulated as a liquid sample microfluidic device [30].

In this paper, a side-polish optical fiber MZI ring laser system based on a micro-taper structure is proposed. The side-polish fiber MZI not only functions as a sensing element, but also can be used as a band-pass filter to obtain a stable and high Q factor spectrum for selecting the laser wavelength. The side-polish fiber MZI was fabricated by a self-built fiber side-polish system. By controlling polish depth, the evanescent field of the optical fiber is enhanced, and the circular symmetry of fiber MZI structure is broken, so as to be used for RI and torsion sensing. A comprehensive study of the RI and torsional response characteristics of the fiber ring laser with different polishing depths fiber MZI are tested and analyzed in detail.

II. THEORETICAL BACKGROUND

When the light in step fiber is transmitted, because it meets the total reflection condition, the light is bound in the fiber core, with very little loss and no interference. Figure 1 shows a schematic diagram of the micro-taper MZI structure, where L is the length of single-mode fiber sandwiched between two micro-tapers, L_1 and L_2 are the length, and D_1 and D_2 are the taper waist diameter of the two micro-tapers. When light is transmitted from a single mode fiber (SMF) to the micro-taper, both core and cladding modes will be excited because of mode field mismatch. Then, the core and cladding mode propagate along the sandwiched SMF and recoupled at the second micro-taper to form MZI. There is a phase difference between the core and the cladding within the sandwiched SMF.

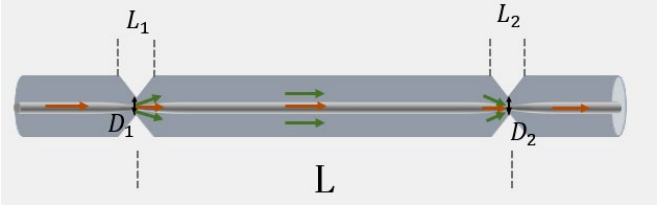

Figure 1. Schematic diagram of the micro-taper MZI structure.

The MZI interference phase difference caused by the optical path difference between the core and cladding modes can be described by [4]:

$$\theta = \frac{2\pi D}{\lambda}(n_c - n_l^j), \tag{1}$$

where, D is the distance between the two taper waists, λ is the wavelength, n_c and n_l^j are the effective indices of the core and j[th]-order cladding modes, respectively. For simplicity, without considering coupling and transmission loss, the interference intensity can be expressed by formula (2):

$$I = I_c + I_l + 2\sqrt{I_c I_l}\cos\theta, \tag{2}$$

where I_c and I_l are the intensity of the core and cladding modes respectively.

Formula (1) clearly shows that wavelength determines the phase difference. The interferometer length D and the effective RI difference (n_c-n_l^j) can determine the periodicity of the interference, and it is expressed by formula (3):

$$\Delta\lambda = \frac{\lambda^2}{D(n_c - n_l^j)}, \tag{3}$$

III. MANUFACTURE OF SENSOR

The micro-taper was made by firstly strip off a 6-cm-long polymer coating of an SMF, a commercial fusion splicer (Fujikura 80C) was using to pull two ends of the SMF when discharge is applied to the bare fiber. In order to prevent bubbling and taper inclination, the setting parameters of fusion splicer are very important. First, select the fusion mode as SM-SM, turn on the switch of cone function, and then set the discharge power and discharge time to + 100 bit and 2000ms, respectively. The waist diameters of the micro-taper is 80 μm as shown in Fig. 2.

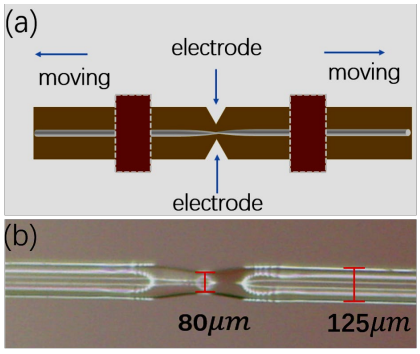

Figure 2 (a) Schematic diagram of fabrication of the micro-taper fiber; (b) Micro-taper points under a microscope.

Figure 3(a) show the self-built fiber side-polishing system. The sandwiched SMF of the fabricated micro-taper structure optical fiber is placed on the grinding wheel adhered with a sandpaper. Both ends of the micro-taper fiber structure were fixed by clamps. The rotation speed of the grinding wheel (about 6cm in diameter) is controlled by a small motor. One end of the micro-taper fiber is connected to a continuous light source, the other end uses an optical power meter(OPM) to monitor the power of the side-polished SMF. First, coarse sandpaper was used for grinding for 15 minutes, at which the speed of the grinding wheel was 180 rpm. Then, fine sandpaper was used for grinding for 40 minutes, and the speed of the grinding wheel was 140 rpm. The corresponding readings of the optical power meter were recorded, and the view of the side polishing area was observed with a microscope and a computer. Then, three different side-polished micro-fiber sensors were fabricated, which marked as W_1, W_2 and W_3 with side-polish depth of 0, 29 and 47 μm, respectively. Figures 3(b) and (c) show the comparison observed by an optical microscope between the side-polished depth with the diameter of single-mode fiber without side-polishing.

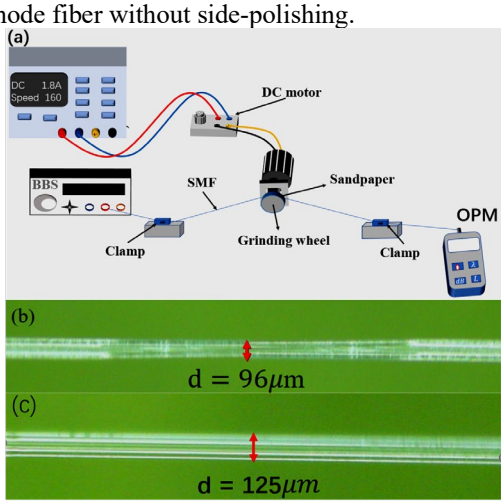

Figure 3 (a) Side polishing platform; (b) Microscope view of the fiber side-polishing section; (c) Microscope view of a single-mode fiber.

IV. EXPERIMENTAL RESULTS

The sensing system of the micro-taper side-polish fiber ring laser is shown in Fig.4. In the system, a 980 nm pump light (VLSS-980-B-650-FA, VENUS) is connected to a 980/1550nm

wavelength division multiplexer (WDM) to input the light source into the cavity. An erbium-doped fiber (EDF, 8/125, Nufern) approximately 5 m long is used as the gain medium of the ring cavity. In order to prevent the return light from damaging the light source, an optical isolator (ISO) is added to the resonant cavity to control the unidirectional propagation of light. The 10:90 optical coupler (OC) outputs 10% of the laser light out of the cavity, and the remaining 90% will circulate in the ring cavity. In addition, in the ring cavity the polarization controller (PC) is inserted inside to adjust the polarization state. When disturbances such as RI and torsional changes are applied to the fiber structure, the phase of the light will change, so that the parameters of the laser cavity are modulated, and the output laser wavelength also changes. A spectrum analyzer (OSA, Anritsu, MS9710C) with a resolution of 0.05 *nm* was used to monitor the wavelength.

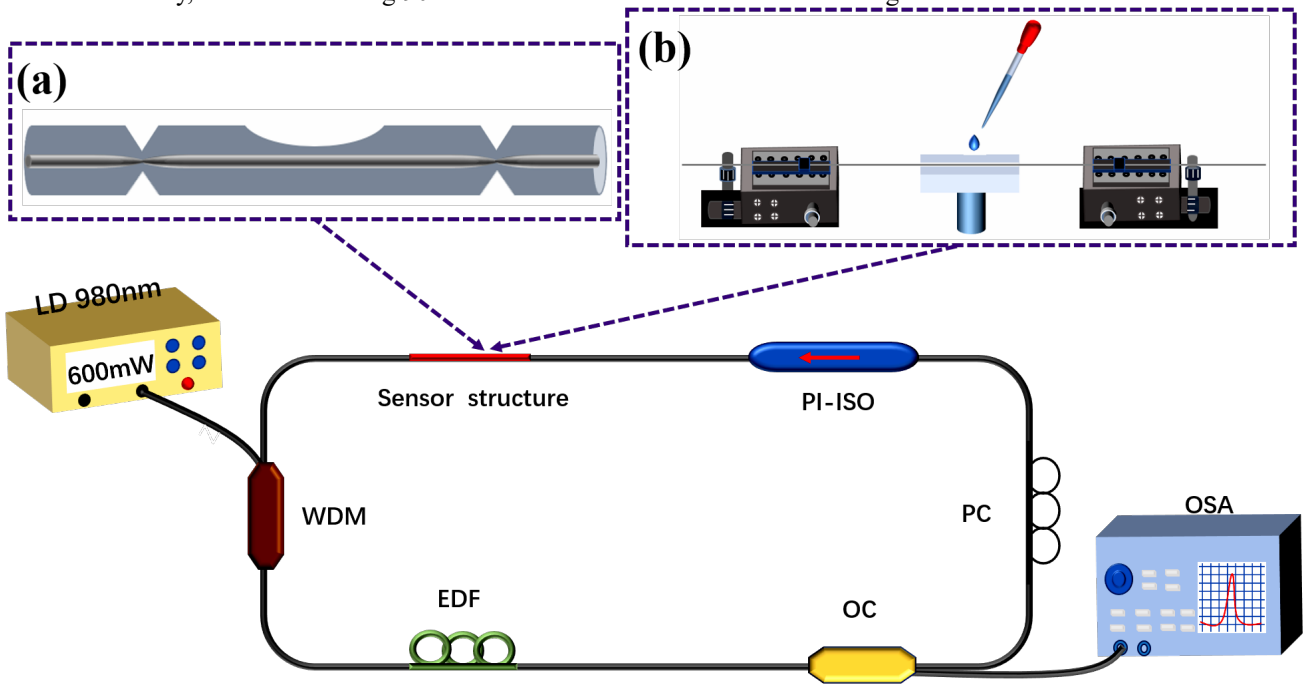

Figure 4. Schematic diagram of fiber ring laser sensor device (inset: a is the MZI sensing structure based on side polishing; b is a diagram of the RI measuring device).

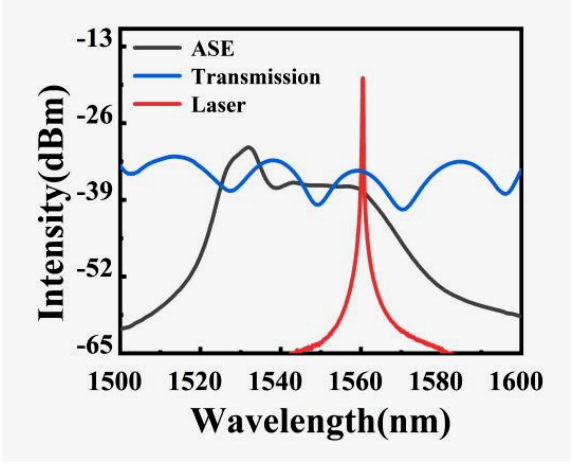

Figure 5. Erbium-doped fiber amplified spontaneous emission (ASE) spectrum; Transmission spectrum of MZI; The output laser spectrum.

The gray line in Fig.5 is the original amplified spontaneous emission spectrum (ASE) of the EDF used in the experiment. The blue line is the transmission spectrum based on the side-polished micro-taper structure MZI, with two peaks in the gain bandwidth from 1525 to 1565 *nm*. When the micro-taper side-polished fiber is combined with a saturated EDF mode-locked resonator, a single wavelength laser of 1560 nm is realized. The red line is the laser spectrum with the FWHM less than 0.15 *nm*.

The setup in Fig.4(b) was used to test the RI of the ring laser system. The pump power and PC are always kept unchanged. the RI response of sensors W_1, W_2 and W_3 with three different side-polishing depths was tested. Figures 6(a)-6(c) show the RI response spectra. As the concentration of RI solution increases, the central wavelength of the laser has an obvious blueshift. Since the absorption loss caused by the increase in the concentration of the refractive index liquid can be compensated by the erbium-doped fiber working in the saturated gain state, so the laser spectrum will only cause the wavelength shift without significant power fluctuations. Fig. 6(d) shows that the RI sensitivity of the micro-taper MZI without side polishing is only -12.695 *nm*/RIU, which is insensitive to the change of external RI. However, the RI sensing sensitivity of W_2 and W_3 after side polishing is increased to -45.67 *nm*/RIU and -81.36 *nm*/RIU respectively. The results show that the RI sensitivity increases significantly with the increase of grinding depth.

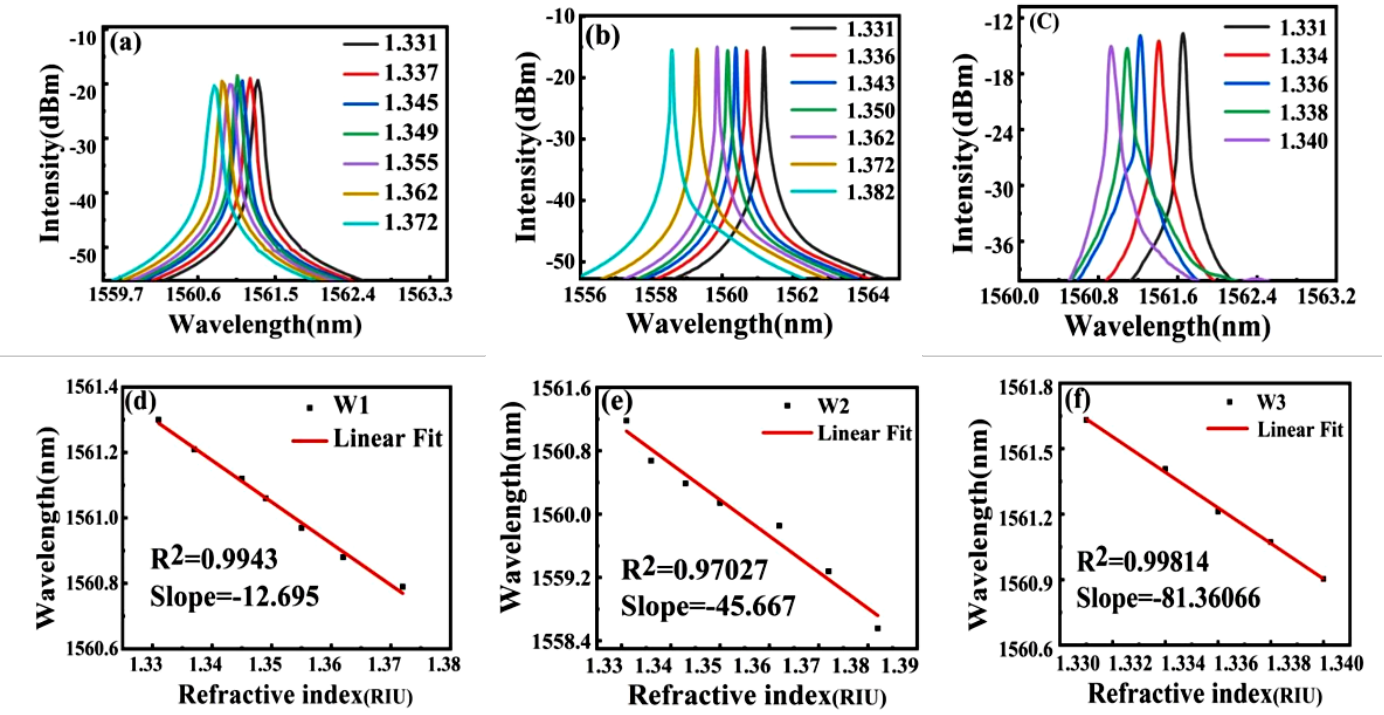

Figure 6. (a)-(c) The RI response spectra of the micro-taper MZI structure with grinding depths of 0, 29, 47μm; (d)-(f) correspond to Linear fitting of the sensing curve.

Figure 7 is a diagram of the system device for measuring the direction twist of the MZI structure. The torsion rate is calculated by the formula $T_r=\omega_0/d$ [18], where $\boldsymbol{\omega_0}$ is the radian corresponding to the rotation angle. During the experiment, the sensing structure is kept straight, and the distance between the two force points is 25.5 *cm*. One end rotates clockwise or counterclockwise through the rotator, and the other end remains fixed. The wavelength change is recorded by changing the rotation angle. The accurate value of the rotating fixture used in the experiment is 5^o, each torsion is changed by 20^o, and the corresponding step length is 1.368 *rad/m*.

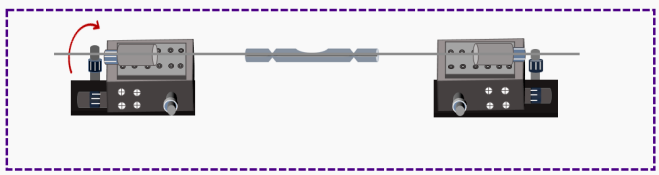

Figure 7. Diagram of experimental setup for torsion measurement.

In addition, the torsional response of sensors W_1, W_2 and W_3 with three different side-polishing depths was tested. In the experiment, only one end of the rotator rotates clockwise, and the pump light source and PC are always kept unchanged. Figure 8 shows the change of the spectrum and the drift of the wavelength with the torsion. During the torsion, only the drift of the wavelength occurs and the peak power is relatively stable. First, turn clockwise from -80^o to 80^o (the T_r range from -5.475 *rad/m* to 5.475 *rad/m*), and the central wavelength of the output laser appears blue shift. Then turn counterclockwise from 80^o to -80^o (the T_r range from 5.475 rad/m to -5.475 r*ad/m*), and the central wavelength of the output laser appears red shift. Experiments show that the sensor has the ability of direction recognition.

Figures 8(a)-8(c) and 8(d)-8(f) are the torsional response spectra and linear fitting diagrams of W_2 and W_3, respectively. The torsional sensitivity of sensors W_2 and W_3 are -0.01 *nm*/^{o} and -0.019 *nm*/^{o}, respectively, the conversion sensitivity to torsional rate is -0.145 *nm*/(*rad.m*$^{-1}$) and -0.267 *nm*/(*rad.m*$^{-1}$), respectively. The results show that the sensitivity of torque increases obviously with the increase of grinding depth. However, the sensor W_1 that has not been side-polished has little effect on it. Because during the torsion test, because the fiber will be affected to a certain extent at the moment of torsion, there will be a short and slight fluctuation in the wavelength at the moment of torsion. But there is no obvious wavelength drift phenomenon.

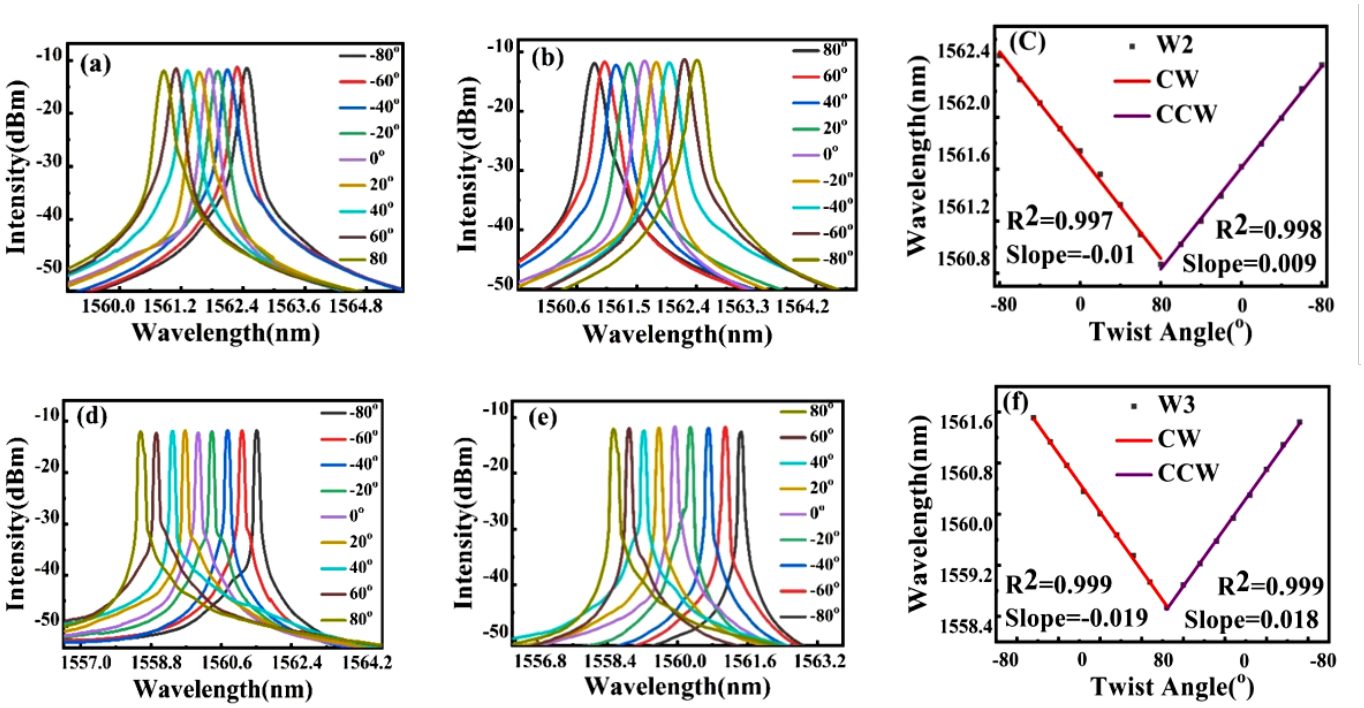

Figure 8. (a)-(c) torsional response spectrum and linear fitting diagram of the micro-taper MZI structures with grinding depth of 29 μm; (d)-(f) torsional response spectrum and linear fitting diagram of the micro-taper MZI structures with grinding depth of 47μm.

TABLE
TABLE 1: COMPARISON OF RI AND TORSION SENSITIVITY WITH DIFFERENT SIDE-POLISHING DEPTHS

Fiber side-polishing depth (μm)	RI sensitivity (RIU)	Torsion sensitivity ($rad.m^{-1}$)
0	-12.695	-
29	-45.667	-0.145
47	-81.360	-0.267

Therefore, the sensor sensitivity tests of MZI fiber ring cavity laser refraction and torsion based on side-polishing are shown in Table 1.

V. CONCLUSION

In summary, an erbium-doped fiber ring laser sensor which is embedded with a side-polishing MZI structure as sensing element and filter, is proposed and experimentally studied. Three fiber MZI samples with different side-polishing depths (0, 29 and 47 μm) were fabricated and introduced into the fiber ring laser, respectively, the RI and torsion sensing characteristics were tested and analyzed in detail. The stable and smooth interference spectrum in the ring laser cavity, with a 3dB bandwidth of less than 0.15 *nm*, enables the laser sensing system to have high measurement resolution and accuracy. Unilateral fiber side polishing process not only effectively enhances the interaction between evanescent wave and external environment, but also breaks the circular symmetry of optical fiber cross section, which can be applied to RI and torsion measurement. In addition, the mechanism that increasing of side-polished depth can greatly improve RI and torsion sensitivities have been demonstrated experimentally. For the side-polishing depth 47 μm, the RI sensitivity reaches -81.36 *nm*/RIU, the torsional sensing sensitivities were achieved -0.019 $nm/^{O}$, the sensitivity converted to torsional rate is -0.267 $nm/(rad.m^{-1})$.

The proposed fiber ring laser sensor has a high Q factor, which makes it has a good measurement resolution. In addition, the side-polished fiber structure reduces fiber diameter only in the side-polishing direction, and is much better than high-sensitivity micro-nano fiber structure in terms of structural strength, which is easy to encapsulate and preserve. It has potential application prospects in in chemistry and biological assays [31,32], motion monitoring and identification [33,34].

REFERENCES

[1] L. Cai, Y. Zhao, X. G. Li, "A fiber ring cavity laser sensor for refractive index and temperature measurement with core-offset modal interferometer as tunable filter," Sensors and Actuators B: Chemical, vol. 242, pp. 673-678, Apr. 2017.

[2] L. Ding, Y. Li, C. Zhou, M. Hu, Y. L. Xiong, Z. L. Zeng, " In-fiber Mach-Zehnder interferometer based on three-core fiber for measurement of directional bending," Sensors, vol. 19, pp. 61-10, Jan. 2019.

[3] T. A. Eftimov, M. Janik, W. J. Bock, "Microcavity in-line Mach-Zehnder interferometers fabricated in single-mode fibers and fiber tapers for visible (VIS) and near-infrared (NIR) operation," Journal of Lightwave Technology, vol. 37, pp. 3351-3356, Jul. 2019.

[4] D. Wang, Y. F. Jiang, X. Geng, B. Yang, L. Li, "Study of asymmetric biconical fiber tapers for in-fiber Mach-Zehnder interferometers and applications in single-frequency fiber lasers," Optics Express, vol. 29, pp. 14384-14393, May. 2021.

[5] X. Lan, J. Huang, Q. Han, T. Wei, Z. Gao, H. Jiang, "Fiber ring laser interrogated zeolite-coated singlemode-multimode-singlemode structure for trace chemical detection," Optics Letters, vol. 37, pp. 1998-2000, June. 2012.

[6] Z. B. Liu, Z. W. Tan, B. Yin, Y. L. Bai, S. S. Jian, " Refractive index sensing characterization of a singlemode-claddingless-singlemode fiber structure based fiber ring cavity laser," Optics Express, vol. 22, pp. 5037-5042, Mar. 2014.

[7] Z. B. Liu, B. Yin, L. Xi, Y. L. Bai, Z. W. Tan, S. Liu, Y. Li, Y. Liu, S. S. Jian, "Axial strain and temperature sensing characteristics of the single-coreless-single mode fiber structure-based fiber ring laser," Applied physics, vol. 117, pp. 571-575, Nov. 2014.

[8] Y. Zhao, L. Cai, X. G. Li, " In-fiber Mach-Zehnder interferometer based on up-taper fiber structure with er3+doped fiber ring laser," Journal of Lightwave Technology: A Joint IEEE/OSA Publication, vol. 34, pp. 3475-3481, Aug. 2016.

[9] J. W. Ma, S. Wu, H. H. Cheng, X. M. Yang, S. Wang, P. X. Lu, " Sensitivity-enhanced temperature sensor based on encapsulated s-taper fiber modal interferometer," Optics & Laser Technology, Vol.139, pp.1-7, Jul. 2021.

[10] Candiani Alessandro, Bravo Mikel, Pissadakis Stavros, Cucinotta, Annamaria, Lopez-Amo Manuel, Selleri Stefano, "Magnetic field sensor based on backscattered intensity using ferrofluid," IEEE Photonics Technology Letters, vol.25, pp.1481-1484, Aug.2013.

[11] H. T. Wang, S. L. Pu, N. Wang, S. H. Dong, J. Huang, " Magnetic field sensing based on singlemode-multimode-singlemode fiber structures using magnetic fluids as cladding," Optics Letters, vol.38, pp.3765-3768, Oct. 2013.

[12] X. Lan, J. Huang, Q. Han, T. Wei, Z. Gao, H. Jiang, "Fiber ring laser interrogated zeolite-coated single mode-multimode-single mode structure for trace chemical detection," Optics Letters, vol. 37, pp. 1998-1999, Jun. 2012.

[13] Z. Yong, Z. Q. Deng, W. Qi, "Fiber optic SPR sensor for liquid concentration measurement," Sensors and Actuators B: Chemical, vol. 192, pp. 229-233, Mar.2014.

[14] Q. Wu, Y. Semenova, P. F. Wang and G. Farrell, "High sensitivity SMS fibre structure based refractometer-analysis and experiment," Optics Express, vol. no. 19, pp. 7937-7944, 2011.

[15] Q. Wu, Y. W. Qu, J. Liu, J. H. Yuan, S. P. Wang, T. Wu, X. D. He, B. Liu, D. J. Liu, Y. Q. Ma, Y. Semenova, X. J. Xin, P. Wang and G. Farrell, "Singlemode-Multimode-Singlemode fibre Structures for Sensing Applications - A Review," IEEE Sensors Journal, vol. 21, no. 11, pp. 12734-12751, 2021.

[16] H. P. Gong, Y. Xiao, N. Kai, C. L. Zhao, X. Y. Dong, "An optical fiber curvature sensor based on two peanut-shape structures modal interferometer, " IEEE Photonics Technology Letters, Vol.26, pp.22-24, Jan.2014.

[17] S. Bing, Y. J. Huang, L. Shen, C. Wang, J. He, C. R. Liao, G. L. Yin, J. Zhao, Y. J. Liu, J. Tang, J. T. Zhou, Y. P. Wang, "Asymmetrical in-fiber Mach-Zehnder interferometer for curvature measurement," Optics Express, Vol. 23, pp. 14596-14602, Jun.2015.

[18] P. Z. Jiang, Q. Y. Yang, H.Y. Guo, A. Zhou, "Highly sensitive torsion senor based on dual-side-hole fiber Mach-Zehnder interferometer," Optics Express, Vol.27, pp.33881-33889, Nov.2019.

[19] Y. Liu, H. C. Deng, L. B. Yuan, "Directional torsion and strain discrimination based on Mach-Zehnder interferometer with off-axis twisted deformations," Optics & Laser Technology, Vol.120, pp.105754. Aug. 2019.

[20] Juan M. Sierra-Hernandez, Arturo Castillo-Guzman, Romeo Selvas-Aguilar, Everardo Vargas-Rodriguez, Eloisa Gallegos-Arellano, Dinora. A. Guzman-Chavez, Julian M. Estudillo-Ayala, Daniel Jauregui-Vazquez, Roberto Rojas-Laguna "Torsion sensing setup based on a three beam path Mach-Zehnder interferometer." Microwave and Optical Technology Letters, Vol.57, pp.1857-1860, Aug.2015.

[21] R. Kumar, Y. K. Leng, B. Liu, J. Zhou, L. Y. Shao, J. H. Yuan, X. Y. Fan, S. P. Wan, T. Wu, J. Liu, R. Binns, Y. Q. Fu, W. P. Ng, G. Farrell, Y. Semenova, H. Y. Xu, Y. H. Xiong, X. D. He and Q. Wu, "Ultrasensitive biosensor based on magnetic microspheres enhanced microfibre interferometer," Biosensors & Bioelectronics, vol. 145, 2019.

[22] Y. J. Wang, S. G. Li, M. Y. Wang, P. T. Yu, "Refractive index sensing and filtering characteristics of side-polished and gold-coated photonic crystal fiber with a offset core," Optics & Laser Technology, Vol.136, pp.1-6, Apr.2021.

[23] C. Y. He, J. B. Fang, Y. N. Zhang, Y. Yu, J. H. Yu, J. Zhang, H. Y. Guan, W. T. Qiu, P. J. Wu, J. L. Dong, H. H. Lu, J. Y. Tang, W. Zhu, N. Arsad, Y. Xiao, Z. Chen, " High performance all-fiber temperature sensor based on coreless side-polished fiber wrapped with polydimethylsiloxane," Optics Express, Vol.26, pp. 9686-9699, Apr.2018.

[24] S. H. Liu, S. Q. Cao, Z. Zhang, Y. Wang, C. R. Chang, Y. P. Wang, "Temperature sensor based on side-polished fiber SPR device coated with polymer," Sensors, Vol.19, pp.1-8, Oct.2019.

[25] X. F. Yang, Bandyopadhyay Sankhyabrata, L. Y. Shao, D. R. Xiao, G. Q. Gu, Z.Q. Song, "Side-polished DBR fiber laser with enhanced sensitivity for axial force and refractive index measurement," Photonics Journal IEEE, Vol.11, pp.1-10, Jun.2019.

[26] W. T. Lin, Y. B. Liu, L. Y. Shao, M. I. Vai, "A fiber ring laser sensor with a side polished evanescent enhanced fiber for highly sensitive temperature measurement, " Micromachines, Vol.12, pp.1-10, May.2021.

[27] J. X. Liu, M. G. Wang, X. Liang, Y. Dong, H. Xiao, S. S. Jian, " Erbium-doped fiber ring laser based on few-mode-singlemode-few-mode fiber structure for refractive index measurement," Optics & Laser Technology, Vol.93, pp.74-78, Aug.2017.

[28] X. K. Bai, D. F. Fan, S. F. Wang, S. L. Pu, X. L. Zeng, "Strain sensor based on fiber ring cavity laser with photonic crystal fiber in-line Mach-Zehnder interferometer," IEEE Photonics Journal, Vol.6, pp.1-8, Aug.2014.

[29] X. J. Xian, X. L. Liu, X. D. Zhang, J. R. Yang, "Dual-ring dual-wavelength fiber laser sensor for simultaneous measurement of refractive index and ambient temperature with improved discrimination and detection limit," Applied optics, Vol.58, pp.7582-7587, Sep.2019.

[30] P. P. Niu, J. F. Jiang, S. Wang, K. Liu, Z. Ma, Y. N. Zhang, W. J. Chen, T. G. Liu, "Optical fiber laser refractometer based on an open microcavity Mach-Zehnder interferometer with an ultra-low detection limit," Optics Express, Vol.28, pp.30570-30585, Oct.2020.

[31] S. Kaushika, A. Pandeya, U. K. Tiwaria, R. K. Sinha. "A label-free fiber optic biosensor for Salmonella Typhimurium detection," Optical Fiber Technology, VOL.46, pp. 95-103, 2018.

[32] M. Mansora, M. H. Abu Bakara, M. F. Omarb, Y. Mustapha Kamilc, N. H. Zainol Abidina, F. H. Mustafad, M. A. Mahdi, "Taper biosensor in fiber ring laser cavity for protein detection," Optics and Laser Technology, VOL.125, pp. 1-7, 2020.

[33] Y. Liua, H. C. Deng, L. B. Yuan, "Directional torsion and strain discrimination based on Mach-Zehnder interferometer with off-axis twisted deformations," Optics and Laser Technology, VOL.120, pp. 1-7, 2019.

[34] M. Yang, L. P. Cooper, N. Liu, X. Q. Wang, M. P. Fok, "Twining plant inspired pneumatic soft robotic spiral gripper with a fiber optic twisting sensor," Optics Express, VOL.28, pp. 35158-35167, 2020.

Wan Bo is a graduate student with the School of Measuring and Optical Engineering, Nanchang Hangkong University. Here she mainly studies the application of erbium-doped mode-locked fiber lasers.

Bin Liu received his B.S. and Ph.D. degree from Sun Yat-sen University, China. Dr. Liu is an associate Professor with Key Laboratory of Nondestructive Test (Ministry of Education) of Nanchang Hangkong University, China. His main research interest is fiber optic sensing.

Juan Liu received her Ph.D. degree from Beijing Normal University, China. She is a lecture with Key Laboratory of Nondestructive Test (Ministry of Education) of Nanchang Hangkong University, China. Her main research interest is fiber optic sensing.

Xing-Dao He was born in Jingan, China, in 1963. He received the Ph.D. degree in optics from Beijing Normal University, Beijing, China, in 2005. He is currently a Professor with the Key Laboratory of Nondestructive Test (Ministry of Education), Nanchang Hangkong University, China. His current research interests include light scattering spectroscopy, optical holography, and information processing.

Jinhui Yuan received the Ph.D. degree in physical electronics from Beijing University of Posts and Telecommunications (BUPT), Beijing, China, in 2011. He is currently a Professor at the Department of computer and communication engineering, University of Science and Technology Beijing (USTB). He was selected as a Hong Kong Scholar at the Photonics Research Centre, Department of Electronic and Information Engineering, The Hong Kong Polytechnic University, in 2013. His current research interests include photonic crystal fibers, silicon waveguide, and optical fiber devices. He is the Senior Members of the IEEE and OSA. He has published over 200 papers in the academic journals and conferences.

Qiang Wu received the B.S. and Ph.D. degrees from Beijing Normal University and Beijing University of Posts and Telecommunications, Beijing, China, in 1996 and 2004, respectively. From 2004 to 2006, he worked as a Senior Research Associate in City University of Hong Kong. From 2006 to 2008, he took up a research associate post in Heriot-Watt University, Edinburgh, U.K. From 2008 to 2014, he worked as a Stokes Lecturer at Photonics Research Centre, Dublin Institute of Technology, Ireland. He is an Associate Professor / Reader with Faculty of Engineering and Environment, Northumbria University, Newcastle Upon Tyne, United Kingdom. His research interests include optical fiber interferometers for novel fiber optical couplers and sensors, nanofiber, microsphere sensors for bio-chemical sensing, the design and fabrication of fiber Bragg grating devices and their applications for sensing, nonlinear fibre optics, surface plasmon resonant and surface acoustic wave sensors. He has over 200 publications in the area of photonics and holds 3 invention patents. He is an Editorial Board Member of Scientific Reports, an Associate Editor for IEEE Sensors Journal and an Academic Editor for Journal of Sensors.